"AIRBLAST ATTENUATION AND FLOW LOSS PERFORMANCE OF PASSIVE ATTENUATORS"

by

Quentin A. Baker
Wilfred Baker Engineering, Inc.
San Antonio, Texas, USA 78209-1128

and

John P. Harrell
Southwest Research Institute
San Antonio, Texas, USA 78238

ABSTRACT

An analytical/experimental program was conducted for Waterways Experiment Station (WES) to develop a passive airblast attenuator to protect hardened shelters from conventional weapon attack. The role of a passive attenuator is to provide protection through attenuation of air shock, which would otherwise enter air ducts, damaging sensitive air filtration and decontamination equipment, electronic and mechanical systems, and injuring building occupants. The design constraints placed on the passive attenuator were that it have no moving parts, be inexpensive, and require no maintenance. Further, air flow loss under normal operating conditions was not to exceed 2.0 in.-H_2O at 500 ft/min. The goal was 99% attenuation of both pressure and impulse.

A Phase I analytical study evaluated the feasibility of using Suppressive Shields concepts for passive attenuators. A series of orifice plates was found to offer less resistance to normal air flow, yet equal or exceed the attenuation levels of any of the Suppressive Shields concepts. The Phase II experimental work included both airblast attenuation and flow loss measurements, and evaluated six concepts, three of which were orifice plate designs. The flow loss requirement proved to be very stringent, and measured losses were greater than analytical predictions. Airblast attenuation levels of 86 to 92% were measured with several orifice plate designs, but with 10 to 14 in.-H_2O pressure drop. Two orifice plate concepts achieved 80 to 85% attenuation of both pressure and impulse at the 2.4 in.-H_2O requirement.

Departing from orifice plate designs in an attempt to improve performance, three concepts were evaluated that directed the shock wave into holding chambers. The best of these designs achieved 87-95% attenuation, with a flow loss of 2.6 in.-H_2O at 500 ft/min.

BACKGROUND

The development of a passive airblast attenuation device for conventional weapons was promulgated by the U. S. Army Engineer Waterways Experiment Station (WES). Active blast valves, designed predominantly for long duration nuclear airblast, have closure times ranging from 1 to 2 ms (Refs. 1, 2). Tests run at WES revealed that such response times are too slow to effectively attenuate the blast from a conventional weapon (Refs. 3, 19). WES conducted full-scale tests using general purpose bombs. Active valves were blocked open during a number of tests, and their performance was compared to tests in which the valve was fully functional. Very little difference

Report Documentation Page

Form Approved
OMB No. 0704-0188

Public reporting burden for the collection of information is estimated to average 1 hour per response, including the time for reviewing instructions, searching existing data sources, gathering and maintaining the data needed, and completing and reviewing the collection of information. Send comments regarding this burden estimate or any other aspect of this collection of information, including suggestions for reducing this burden, to Washington Headquarters Services, Directorate for Information Operations and Reports, 1215 Jefferson Davis Highway, Suite 1204, Arlington VA 22202-4302. Respondents should be aware that notwithstanding any other provision of law, no person shall be subject to a penalty for failing to comply with a collection of information if it does not display a currently valid OMB control number.

1. REPORT DATE	2. REPORT TYPE	3. DATES COVERED
AUG 1992		**00-00-1992 to 00-00-1992**

4. TITLE AND SUBTITLE	5a. CONTRACT NUMBER
Airblast Attenuation and Flow Loss Performance of Passive Attenuators	5b. GRANT NUMBER
	5c. PROGRAM ELEMENT NUMBER
6. AUTHOR(S)	5d. PROJECT NUMBER
	5e. TASK NUMBER
	5f. WORK UNIT NUMBER
7. PERFORMING ORGANIZATION NAME(S) AND ADDRESS(ES) **Wilfred Baker Engineering, Inc., ,San Antonio,TX,78209-1128**	8. PERFORMING ORGANIZATION REPORT NUMBER
9. SPONSORING/MONITORING AGENCY NAME(S) AND ADDRESS(ES)	10. SPONSOR/MONITOR'S ACRONYM(S)
	11. SPONSOR/MONITOR'S REPORT NUMBER(S)

12. DISTRIBUTION/AVAILABILITY STATEMENT
Approved for public release; distribution unlimited

13. SUPPLEMENTARY NOTES
See also ADA260985, Volume II. Minutes of the Twenty-Fifth Explosives Safety Seminar Held in Anaheim, CA on 18-20 August 1992.

14. ABSTRACT
see report

15. SUBJECT TERMS

16. SECURITY CLASSIFICATION OF:			17. LIMITATION OF ABSTRACT	18. NUMBER OF PAGES	19a. NAME OF RESPONSIBLE PERSON
a. REPORT **unclassified**	b. ABSTRACT **unclassified**	c. THIS PAGE **unclassified**	**Same as Report (SAR)**	**21**	

was seen between the performance of active and blocked valves. Furthermore, some types of the active valves failed to operate properly under repeated high blast pressures from conventional weapons. These valves were found to be relatively fragile, deforming and seizing shut.

A passive airblast attenuation device that contains no moving parts is attractive because of its potential as a rugged, low cost, low maintenance item. Active valves may be the weak link in a facility under a multi-hit attack or at loads higher than design pressure. Further, the active valves must be cleaned to ensure that dirt, sand, or other particles do not interfere with the motion of a moving component, or prevent proper seating of the valve. The maintenance, reliability, and fragility problems associated with active valves are eliminated with a passive attenuator.

A Phase I study was completed in October of 1989 (Ref. 4). The concepts evaluated in Phase I were based on the Suppressive Shields program, which was active in the mid 1970's (Refs. 5-13). The Suppressive Shields program developed, analyzed, and tested a number of concepts for fixed, vented panels and structures. All vented panels were intended to strongly attenuate airblast from an internal detonation, and to arrest high speed fragments. The suppressive shields concepts were:

1. nested angles,
2. side-by-side angles or zees,
3. louvers,
4. interlocking I-beams, and
5. perforated plates.

A passive device consisting of a series of perforated plates was analyzed thoroughly. Shock tube data (Refs. 6, 15) were used to develop a design curve for peak pressure attenuation using a series of perforated plate with equal vent area per plate. A similar design curve was developed for impulse attenuation based on WES experiments (Ref. 18). The WES data showed impulse attenuation through perforated plates was generally not as great as pressure attenuation. It must be noted that it was assumed that single-plate data could be applied to a series of multiple plates, as recommended in References 9 and 10, but no test data existed during the Phase I study to verify this assumption. Phase II tests have subsequently proven this assumption to be false. The interaction of shock between plates reduces the effectiveness of the second and subsequent plates. As a result, the Phase I study overpredicted the attenuation of peak pressure.

The Phase I study analyzed flow loss through a perforated plate passive attenuator. A significant finding of this study was that flow loss through a plate with many perforations is significantly greater than that of a single orifice plate of equivalent vent area. Since shock tube tests show that pressure attenuation was independent of the perforation pattern as long as the holes were of larger diameter than plate thickness (Refs. 6, 14, 15), the Phase I study recommended a single orifice per plate, with the orifices offset to diagonally opposite corners of a square plate.

Nested angles, side-by-side angles or zees, louvers, and interlocking I-beams were also studied. Attenuation predictions were limited to peak pressure due to a lack of impulse attenuation concerning these devices. The Suppressive Shields data were the basis for peak pressure attenuation predictions in all cases (5-13). Flow loss calculations were also very limited due to the lack of empirical data for these geometries. However, it was readily apparent that flow losses through these devices would be higher than an orifice plate of equivalent vent area, and that attenuation through the perforated plates would be superior.

DESIGN CONSTRAINTS

The following are the design constraints imposed on the passive attenuator:

1. Pressure attenuation of 100:1 or greater
2. Impulse attenuation of 100:1 or greater
3. Air flow restriction of 2.0 in.-H_2O or less at 500 ft/min
4. No maintenance
5. Low cost
6. Applicable to new as well as existing facilities

Missing from the list of design constraints is delineation of the size of the duct to which a passive attenuator will be coupled. The approach taken was that all passive devices have the same cross-sectional area as the downstream duct. This approach prohibited use of a passive device that was larger than the mating duct's area, or use of multiple passive devices that are collectively larger than a duct, to meet the flow loss design constraint. The latter approach is commonly employed with active blast valves (Refs. 1, 2).

Requiring passive attenuator cross-sectional area to equal duct area is a very stringent constraint. But, the small size will be beneficial in the design of protective structures by minimizing the area of the exterior opening as well as the internal building volume occupied by the device.

Pressure Drop Test Apparatus

The pressure drop characteristics of air flowing through the passive attenuators was determined using a specially constructed wind tunnel. The design of the tunnel, illustrated in Figure 1, was based on the recommendations of ANSI/AMCA Standard 210-85 (ANSI/ASHRAE Standard 51-1985) *Laboratory Methods of Testing Fans for Rating.* The tunnel consists of three sections. The first was an 8-ft-long entrance section with a 2 x 2-ft cross-section. The blast valve model to be evaluated was positioned in this entrance section for testing. A flow straightening screen was located midway in the entrance section. This screen broke up any large scale turbulence caused by the flow through the blast valve. The entrance section opened into a central plenum chamber 8-ft long, with a cross-section of 4 x 4-feet. The chamber was divided in half by a central bulkhead that was penetrated by three ASME long radius flow nozzles, two each with 6-inch throat diameters, and one with a 5-inch throat. Upstream and downstream of the flow nozzles and bulkhead were flow straighteners consisting of 3/8-in. aluminum honeycomb and fine mesh wire screens. The central chamber was connected to a 4-ft long tail section with a 2 x 2-ft cross-section. A large centrifugal blower was connected to the end of the tail section to pull air through the tunnel. The blower was powered by a directly coupled 15 HP hydraulic motor. Blower speed and flow rate were controlled by a flow control valve on the hydraulic supply line to the motor.

Tunnel instrumentation included a magnetic pick-up, 60-tooth gear and frequency counter for measuring blower rpm; a thermocouple and digital display for measuring entrance section air temperature; and Magnehelic® gauges and an inclined 6-inch manometer for measuring differential pressures. The Magnehelic gauges were used for preliminary tests and rough pressure measurements, and the manometer used for final testing because of its superior accuracy and resolution. Flush-wall pressure taps were used to measure pressures upstream and downstream of the nozzle bulkhead. Pressures downstream of the test article in the entrance section were taken by a static probe extending into the flow and located behind the flow straightening screen in the entrance section.

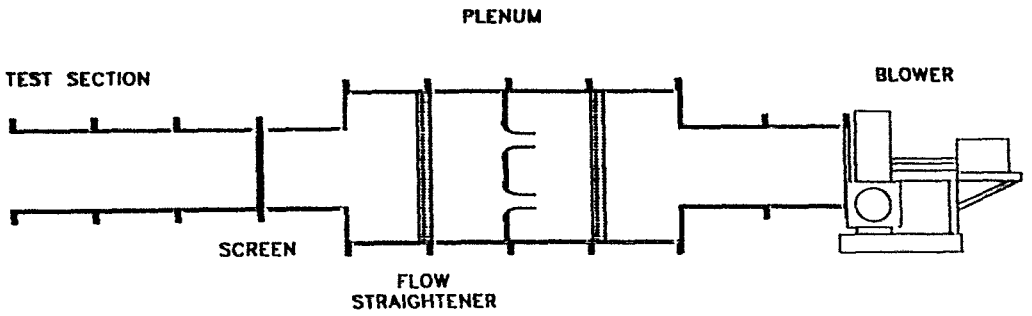

Figure 1. Schematic of Pressure Drop Test Apparatus

The data were analyzed following the recommended procedures and formulations in ANSI/AMCA Standard 210-85. An iterative procedure was used to calculate total flow through the wind tunnel using the combined throat areas of the ASME flow nozzles in use, barometric pressure, wet and dry bulb temperatures, and the pressure drop across the nozzles as inputs. Actual flow rates through the tunnel were calculated; then the average flow velocity using the cross-sectional area of the attenuator under test was determined. Finally, a least-squares second order curve was fit through the data, and produced a graph of the results in the form of air velocity versus pressure drop curves.

Airblast Attenuation Test Fixture

The test apparatus for airblast attenuation measurements was designed to evaluate performance of a passive device mounted flush in an external wall of a structure. The apparatus had three main components: a wall, a tunnel, and a passive device.

The wall consisted of a 6 X 5 X 2.5-ft reinforced concrete, steel clad block. The width and height of the wall's front face were designed to allow sufficient time for completion of the positive phase before rarefaction waves reached the passive attenuator.

The tunnel measured 28 ft long, and was fabricated from 12 X 12 X 1/4-in. square steel tube. It served several purposes. Its cross-sectional size was identical to that of all passive attenuators, thus eliminating expansion or compression of a shock exiting an attenuator. The length of the tunnel was selected based on shock-tube data which indicated that shock waves disturbed by an orifice plate will coalesce within a distance of seven tube diameters from the plate (Refs. 14, 15). An internal gage was conservatively placed 13 diameters downstream of the front face of the attenuator in the tunnel. The remaining 15 ft of tunnel downstream from the gage acted to delay the arrival of the external shock entering through the open end of the tunnel.

The wall and connected tunnel are shown in Figure 2. Each passive attenuator was designed to fit within the cavity depicted in the vertical cross-section shown in Figure 2. The center of the 12 x 12-in. attenuator opening was positioned level with the charge, 10 in. above ground level. Placement of the opening at this position was accomplished by burying the wall 14 in., as shown in Figure 2.

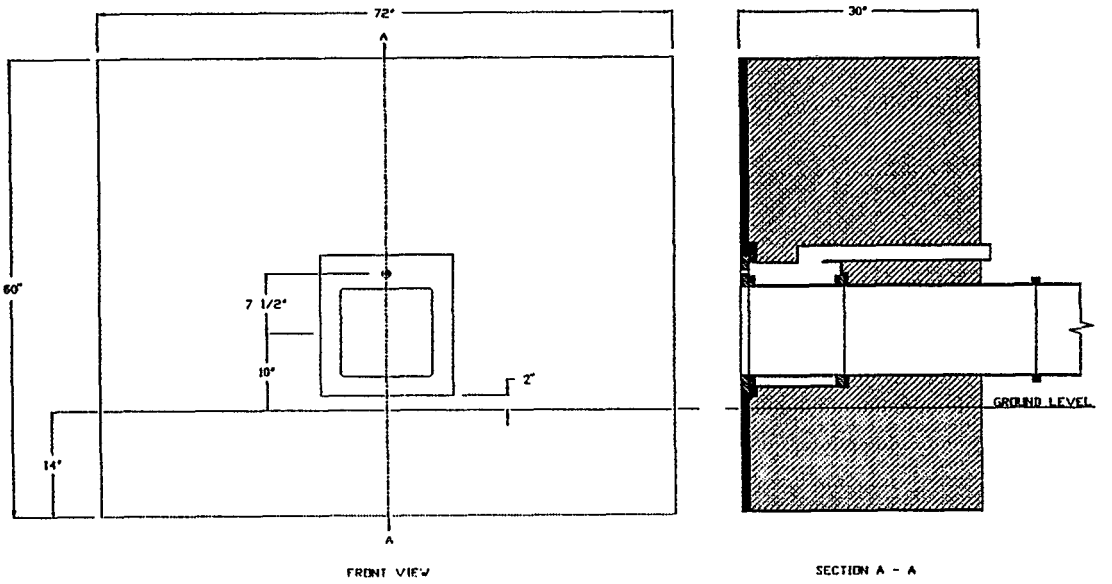

Figure 2. Airblast Attenuation Test Fixture

It was necessary to account for shock decay as the shock traveled down the tube. This was accomplished by baselining the tunnel without a passive attenuator installed. An empty housing of the same internal dimensions (11.5 X 11.5 in.) as the tunnel was substituted for a passive device during baseline tests. The ratio of tunnel pressure to incident pressure was calculated at each standoff. The same ratio was calculated for each passive device and divided by the baseline pressure ratio to determine pressure attenuation percentage. The formula developed was:

$$Pressure\,Attenuation = \left[1 - \frac{(P_T/P_1)_{attenuator}}{(P_T/P_1)_{baseline}}\right] \times 100$$

where P_1 is the reflected pressure at the external opening of the passive attenuator and P_T is the side-on pressure measured 13 ft downstream of the attenuator entrance. The formula calculates the attenuation directly attributable to the passive attenuator, with the effects of unrestricted opening size and tunnel length not being credited to the attenuator's performance. Impulse attenuation was calculated in a similar manner.

Two-pound, Composition B spherical charges were used in all tests. Two standoffs were selected for testing. Horizontal standoffs of 48 and 77 in. from the charge to the front face of the wall produced reflected pressures of 200 and 850 psi, respectively, at the openings of the test attenuators.

Reflected blast pressure on the front face of the attenuator was measured using 1,000 psi PCB Model 102A flush-mounted quartz pressure transducers. This transducer was mounted on the vertical centerline and 7 1/2-in. above the centerline of the attenuator.

Blast pressure downstream of the attenuator was measured with a PCB pencil gage mounted on the end of a 15-ft long, 3/4-in. PVC pipe inserted into the tunnel from the open end. The pipe and gage were supported by two sets of double-legged PVC braces. Both the pipe and bracing acted to isolate the gage from tunnel vibration. Pressure levels measured by the pencil gage varied with different attenuator configurations. A PCB 137A12 pencil gage was used when expected pressures were between 5 psi and 50 psi. A PCB 137M15 pencil gage was selected for expected pressures below 5 psi. The sensing element of the pencil gage was positioned 13 ft downstream of the front face of the passive devices.

Pressure signals were amplified using a PCB Model 483B07 amplifying power unit. A LeCroy 6810 digitizing system converted the data to digital form. The pressure data were sampled at a rate of one reading per microsecond. A total of 131,072 data points were recorded per channel per test, providing 0.131 second of data.

Baseline Airblast Attenuation

Baseline tests were conducted with 2-lb spherical charges at a 48-in. standoff to determine the charge height required to fully form a Mach stem at the height of the pressure transducer located directly above the opening to each passive attenuator. A fully formed Mach stem at the entrance to the attenuator was more desirable than multiple peak traces to avoid analysis of complicated pressure traces. A charge height above ground of 11 in. was found to be the upper limit. A 10-in. charge height was selected for testing.

Baseline tests were also conducted to provide reference data for evaluation of attenuator performance. Test results are shown in Table 1.

Table 1. Average Baseline Test Data

	Incident		13 Ft Down Tunnel			
Charge Standoff (in.)	P_r Reflected Pressure (psi)	i_r Reflected Impulse (psi-ms)	P_s Side-On Pressure (psi)	i_s Side-On Impulse (psi-ms)	P_s/P_r	i_s/i_r
48	782.1	91.11	22.78	33.28	0.293	0.3656
77	183.6	55.67	13.26	22.32	0.722	0.4033

Orifice Plate Passive Attenuators

The orifice plate design recommended as a result of the Phase I study (Ref. 4) is depicted in Figure 3. It consisted of six parallel orifice plates measuring 29.5 in. X 29.5 inches. The orifice in each plate had a radius of 4.25 in., which provided 6.25% vent area per plate. The orifices were offset to diagonally opposite corners from plate to plate.

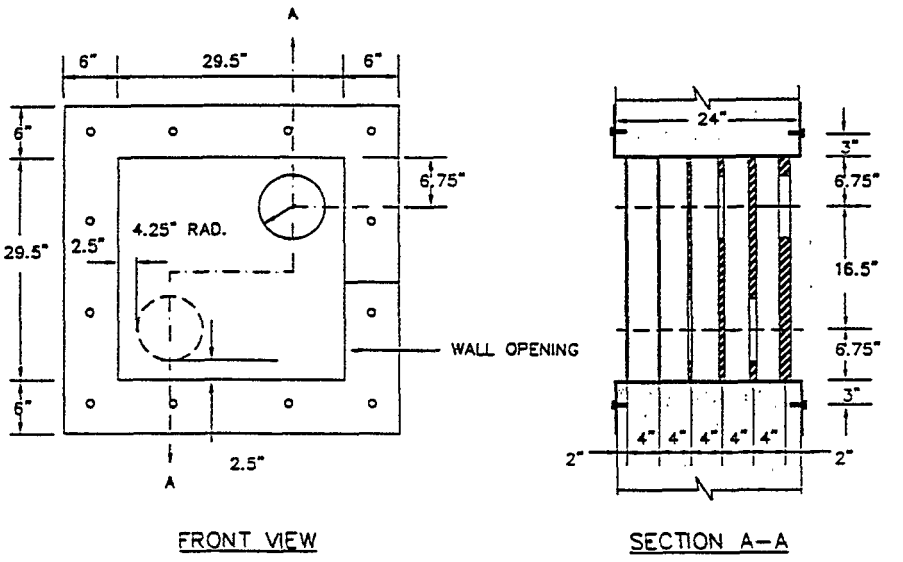

Figure 3. Six-Plate Orifice Device with 6.25% Vent Area

Pressure drop tests were conducted with the number of orifice plates being varied from a single plate to six plates. Plate positioning was as shown in Figure 3. The results of this series of tests are illustrated in Figure 4. This model demonstrated a high pressure drop at low flow velocities, with even the single plate with 6.25 percent open area exceeding 2.0 in.-H_2O of water pressure drop at just over 200 ft/min.

For the next series, the open area of each orifice plate was increased to 12 percent. In this series, only five plates were used, and the spacing between plates was adjusted in 1-in. increments between 2 in. and 8 inches. Figure 5 shows the results of this test series. The pressure drop with the larger open area was far superior to that at the 6.25 percent open area model, but still far short of the required level of performance. The results also show that plate spacings larger than 4 in. have negligible effect on pressure drop. Only as the plate spacing moves below four inches does performance begin to deteriorate. This is instructive since the cross-sectional flow area between plates at a 4-in. spacing is equivalent to a 17.8 percent open area for flow, far larger than the 12 percent open area of the orifice plates themselves. The deteriorating performance of the model as plate spacing was moved closer than 4 in. is attributed to the increasingly sharp turns the flow must negotiate.

Airblast attenuation tests involved a smaller version of the six-plate device described above, with the plates measuring 1 ft X 1 ft. Orifice size was 6.25%. The device was initially tested with only the first plate. Subsequent plates were added one at a time. Two repeat tests were conducted at 48- and 77-in. charge standoffs for each of the six configurations.

The results of airblast attenuation tests with 6.25% orifice plates are presented in Figures 6 and 7. These figures indicate that the addition of each plate improved attenuation, but the sixth

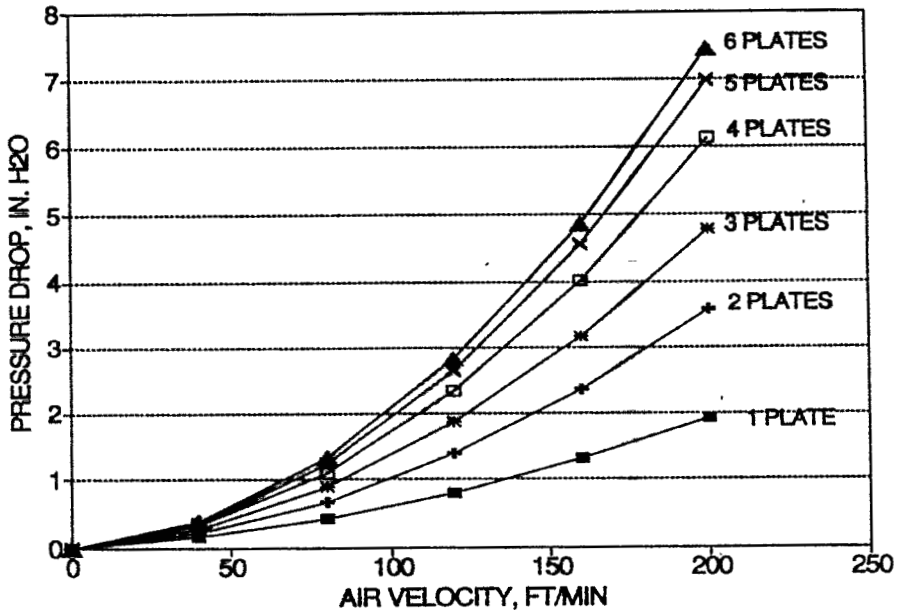

Figure 4. Pressure Drop Through Offset Circular Orifice Model, 6.25% Open Area, for Various Numbers of Plates, 4-In. Plate Spacing

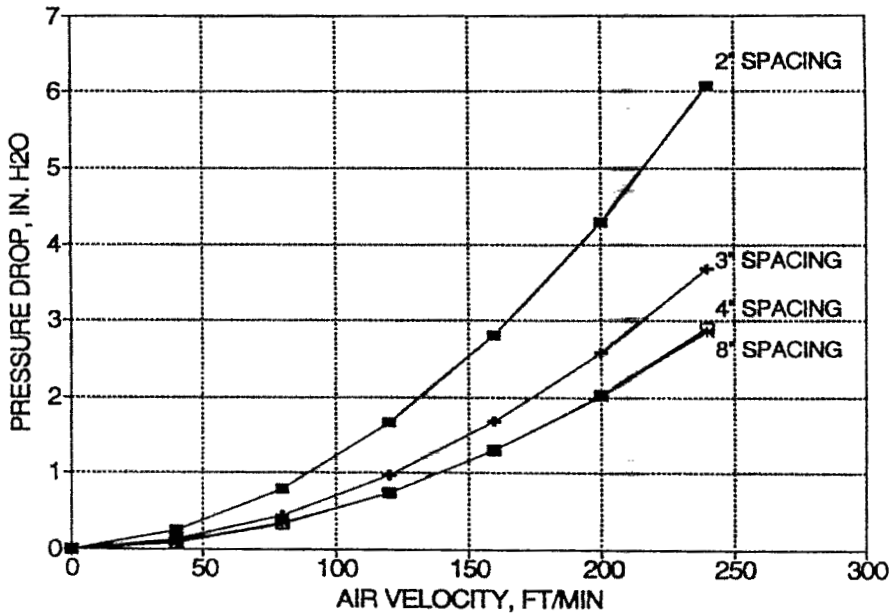

Figure 5. Pressure Drop Through Five-Plate Offset Circular Orifice Model, 12% Open Area, at Various Plate Spacings

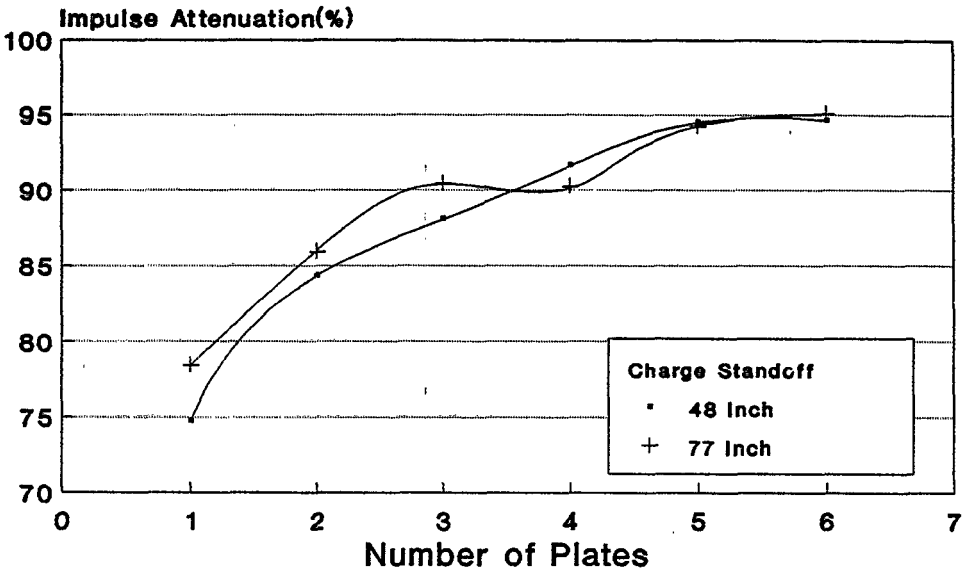

Figure 6. Impulse Attenuation Comparison of 6.25% Vent Area Orifice Plate Attenuator

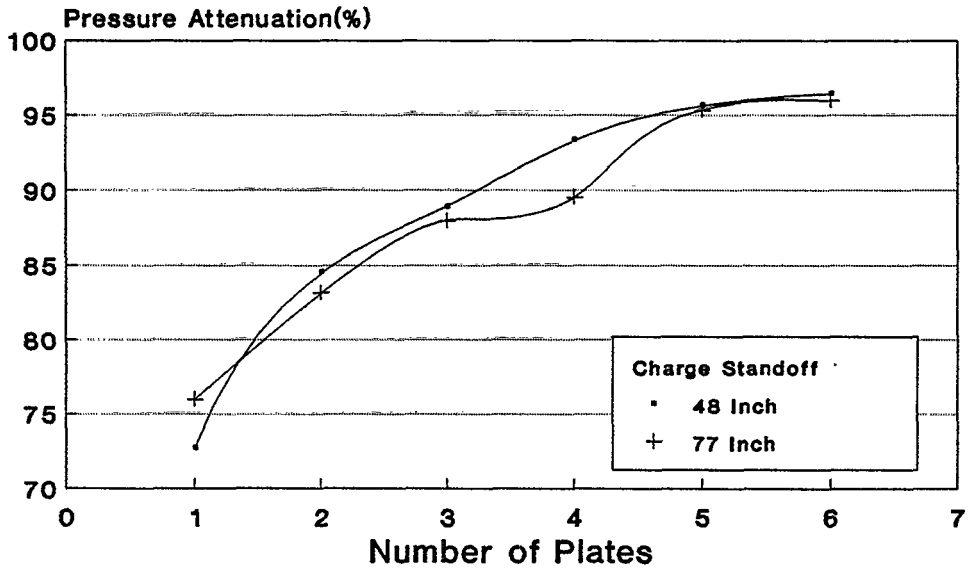

Figure 7. Pressure Attenuation of 6.25% Vent Area Orifice Plate Attenuator

plate made only a slight improvement. Attenuation performance with five plates was quite good, reaching essentially 95.5% pressure and 94.3% impulse attenuation at both charge standoffs. The sixth plate only marginally improved attenuation, the gains being less than 1 percentage point.

The sixth plate is of questionable value based on these results. A penalty is incurred in flow loss with the sixth plate, with very minimal attenuation improvement.

Pressure attenuation predictions made during Phase I for the second and subsequent plates greatly exceeded the measured performance. Clearly, the assumption that single-plate shock tube data could be used for multiple plates in succession was not valid for a six-plate, 6.25% vent area configuration.

The above tests revealed that larger orifice sizes and/or small numbers of plates would be required to meet the flow loss design constraint. The orifice size and number of plates were varied until it was ascertained that a four-plate, 31% vent area model would meet the flow requirement. This large vent area necessitated the use of rectangular orifices, offset from side-to-side as shown in Figure 8.

As before, the test series with 31% orifice plates consisted of test runs at various plate spacings, ranging from 5 to 9 inches. The results of this series are shown in Figure 9. Pressure drop measured at 500 ft/min was 2.7-in. H_2O with the 9-in. plate spacing.

Airblast attenuation test results for the 31%, four-plate device design are presented in Figures 10 and 11 as a function of plate spacing. The 4-in. plate spacing equates to a total depth for the device of 1 ft, which is the same overall depth of the 6.25%, six-plate configuration. Peak pressure attenuation for the 4-in. plate spacing was 82.9 and 81.1% at the 48- and 77-in. standoffs, respectively. The corresponding impulse attenuations were at 77.2 and 81.0%.

Increasing plate spacing of the 31%, four-plate configuration reduced attenuation, particularly impulse, which fell from 81.0 to 66.6% at the 48-in. charge standoff at plate spacings of 4 and 12 in., respectively, as shown in Figure 11.

It was concluded that orifice plate spacing should be at the minimum spacing that is acceptable from a flow loss standpoint. In general, this spacing will be about 1.5 times the orifice width for a rectangular orifice.

Device 3, shown in Figure 12, represented a departure from the Suppressive Shields or orifice plate concepts. Tests of orifice plate configurations revealed that large orifice sizes would be required to meet the flow loss design constraint, and that shock attenuation of 80 to 83% was the best that could be expected. Device 3, and later Devices 5 and 6, were developed to have improved flow characteristics and shock attenuation performance compared to orifice plates. These three devices no longer relied upon a series of restrictions to attenuate shocks. Rather, they directed shocks into holding chambers, which redirected the reflections toward the entrance.

Device 3 relies upon four chambers to accept and expand a blast wave, with reverse flow being directed at a shallow angle toward the front of the device. A blast wave enters through a 6.5% orifice in the front plate of Device 3. Each of the four chambers has a vane which directs approximately 2/3 of the blast wave into a chamber, with the balance passing through a 6.5% (of frontal area) passage. A rear orifice plate was positioned downstream of the four chambers, which also had a 6.5% orifice.

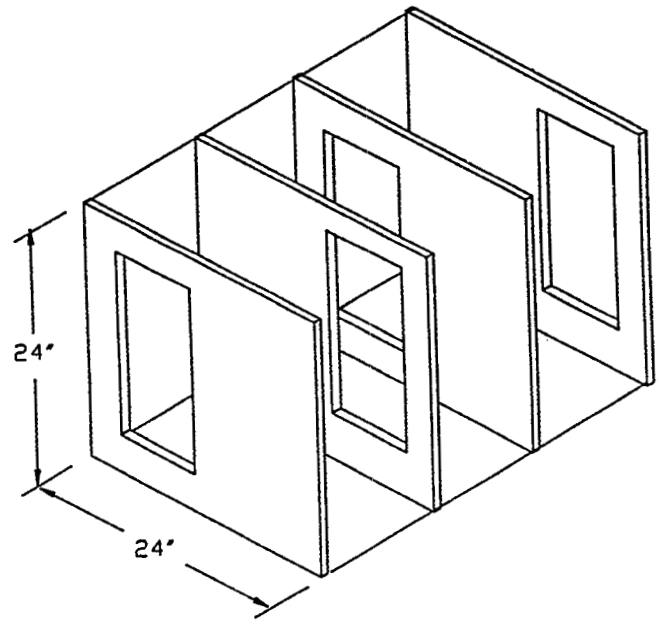

Figure 8. Configuration of Four-Plate Rectangular Orifice Model

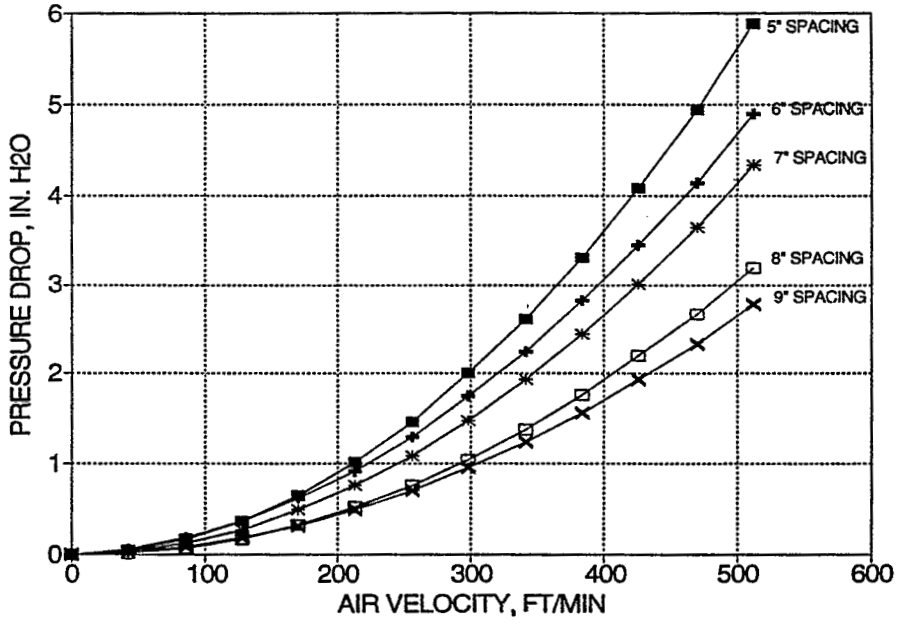

Figure 9. Pressure Drop Through 2 X 2-ft Four-Plate Rectangular Orifice Model, 31% Open Area, for Various Plate Spacings

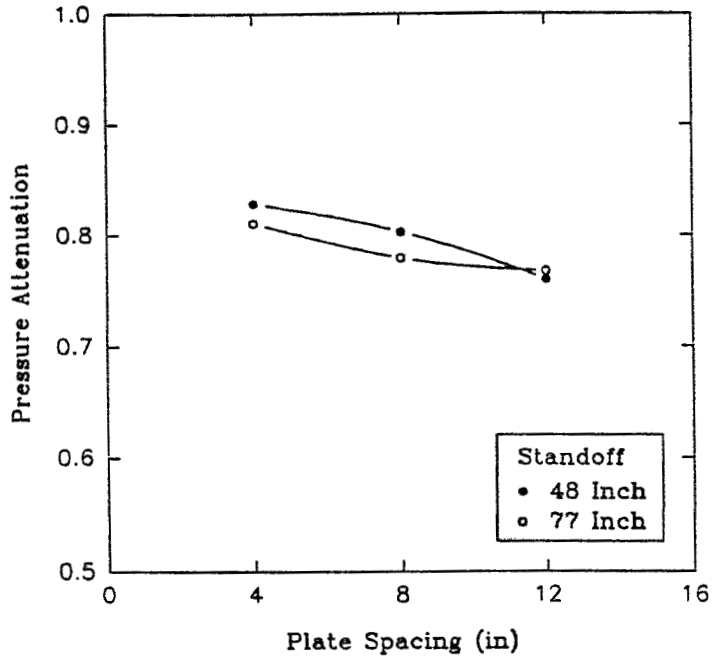

Figure 10. Effect of Plate Spacing on Pressure Attenuation; 31%, Four-Plate 1 X 1-ft Rectangular Orifice Model

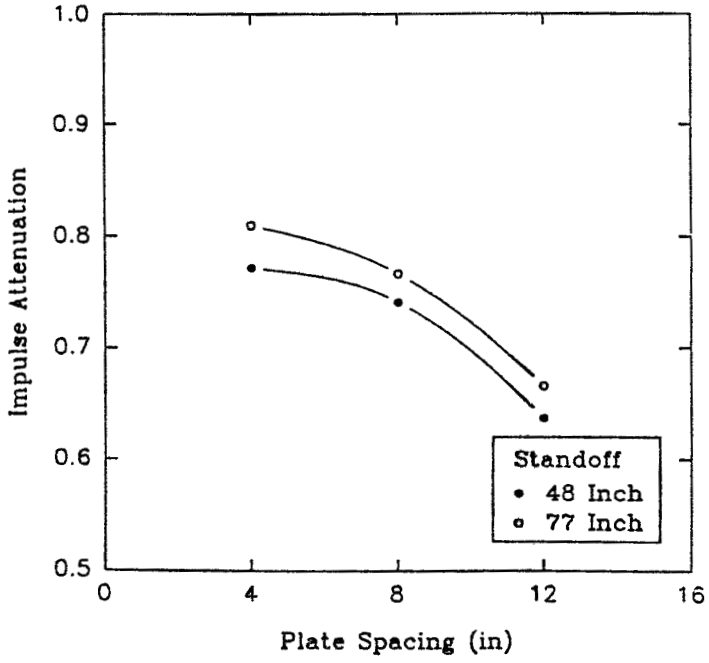

Figure 11. Effect of Plate Spacing on Impulse Attenuation; 31%, Four-Plate 1 X 1-ft Rectangular Orifice Model

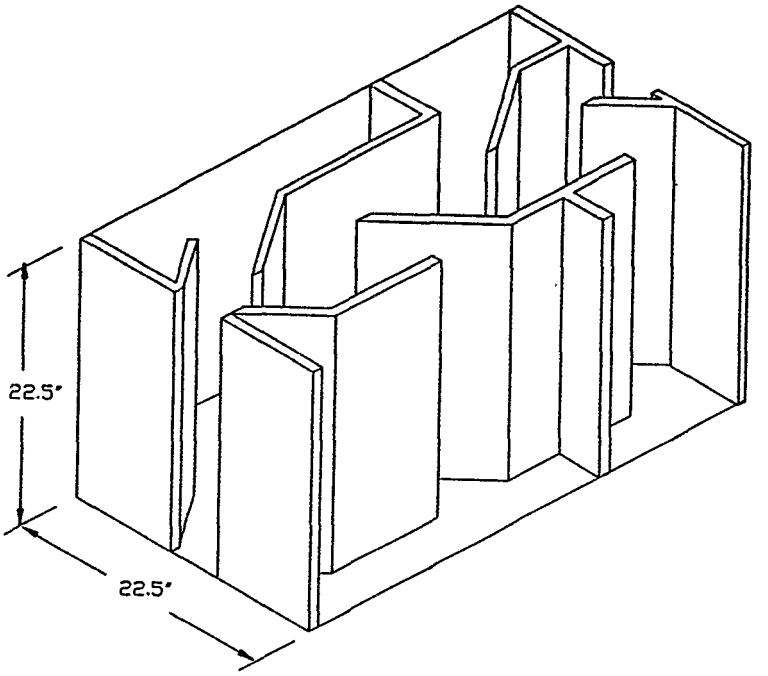

Figure 12. Configuration of Device 3 (Top and Right Walls Removed)

A 12% vent area version of Device 3 was also developed. This was accomplished by doubling the dimensions of the center vane assembly, which made it twice the width and length shown in Figure 12. The width and height of the housing were not increased; consequently, the wider vane assembly reduced the width of the chambers. This loss in chamber width was made up by increased chamber length, with the final chamber volumes being essentially the same as the 6.5% vent area model.

Flow loss tests were conducted on both the 6.5 and 12.0% Device 3 models, but only the 6.5% design was subjected to airblast attenuation tests. Airblast attenuation tests were not conducted with the 12% model when it was found that the more restrictive 6.5% model would not meet the 100:1 attenuation goal.

The results of the pressure drop tests are shown in Figure 13. Even though the 12 percent open area model performed significantly better than the 6 percent open area model, its performance was not as good as the 12%, six-plate orifice model (with plate spacings greater than 4 in.). This disappointing result is attributed to the internal turbulence and flow separation in the device as the flow passes around the internal baffle plates.

The results of airblast attenuation tests of Device 3, conducted with the 6.5% vent area design, are presented in Table 2. Shock attenuation was almost identical for the two charge standoffs (48 and 77 in.). Peak pressure and impulse were reduced by essentially 95 and 93%, respectively. These values are very close to those of the six-plate 6.25% orifice plate attenuator measured at the 77-in. charge standoff. Thus, Device 3 did not achieve the desired improvements over orifice plate designs.

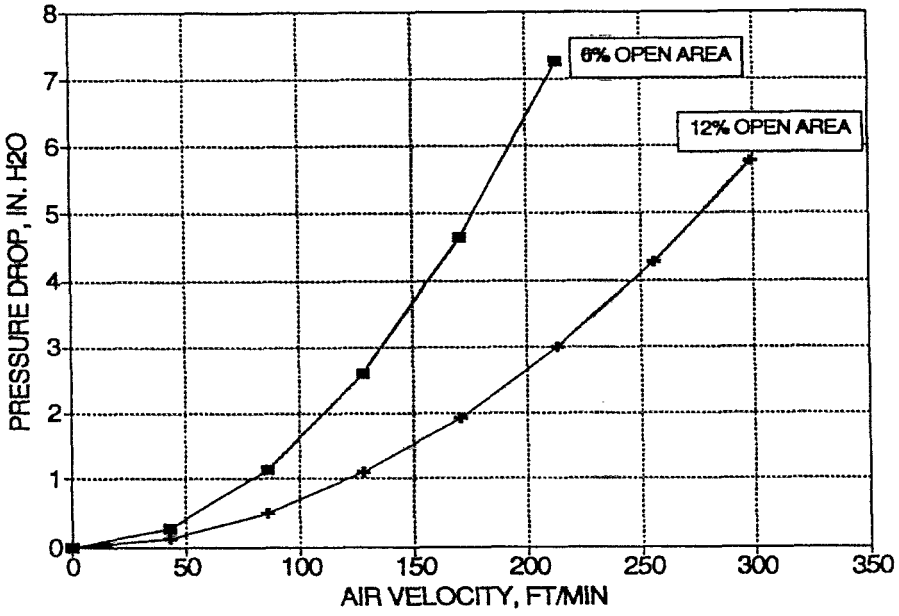

Figure 13. Pressure Drop Through Device 3 with 6% and 12% Open Areas

Table 2. Performance of 6.5% Vent Area Device No. 3

Shock Attenuation (%) 48-In. Standoff		Shock Attenuation (%) 77-In. Standoff	
Pressure	Impulse	Pressure	Impulse
96.3	93.7	95.2	94.0

Device 5, shown in Figure 14, consists of a series of angled plates, which, like Device 3, direct shocks to the sides and away from the opening to the next chamber. The shallow angle between plates reflects shocks toward the front of the device. The clearance between the tip of one plate and the side of adjacent plate controls flow area. Device 5 was subjected to flow loss tests first, where its design was optimized to meet the flow loss design constraint. Subsequently, the optimized design was subjected to airblast attenuation tests.

Two versions of Device 5 were flow loss tested: a 12% open area version, and a 31% open area version. The vent area through all restrictions was identical within these two models. As expected, the 31% open area model had significantly less pressure drop than the 12% open area model. Though sharing similarities with Device 3, Device 5 demonstrated much lower pressure drop, even with smaller open areas.

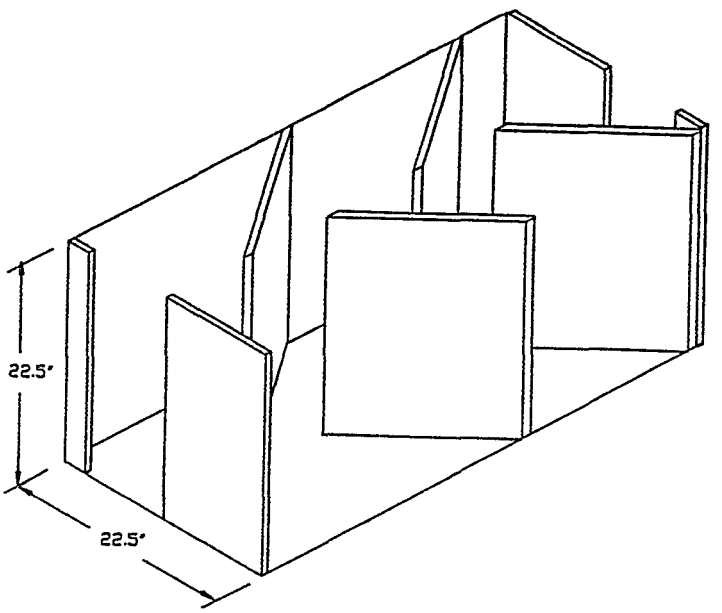

Figure 14. Configuration of Device 5 (Top and Right Walls Removed)

The 31% version of Device 5 was modified to include internal turning vanes to direct flow around the tip of each plate, as depicted in Figure 15. Figure 16 summarizes the results of the tests of the three versions of Device 5. The 31% open area model with turning vanes was very close to the performance standards established for the blast valve, with a pressure drop at 500 ft/min of 2.3 in.-H_2O.

The rear plate of Device 5 was removed, and the front opening width was varied to further reduce flow loss. It was determined that a 17.8% vent in the front plate, 31% open area at the tip of each internal plate, and no rear orifice plate would exactly meet the 2.0 in.-H_2O at 500 ft/min requirement. This configuration was subjected to airblast attenuation tests.

The results of airblast attenuation tests are presented in Table 3. The 77-in. standoff produced the best performance, with pressure being attenuated by 83.6% and impulse by 80.9%. These figures are essentially the same as the 31% four-plate orifice device. The turning vanes, necessary to achieve good air flow characteristics, could be the reason for the attenuation shortcomings.

The design of Device 6, shown in Figure 17, was formulated based on the cumulative knowledge from the previous attenuators. Device 6 relies upon a single chamber or "shock trap" to accept the incident shock and redirect it out the front opening. Tests with Device 3 identified the need for such a large chamber. Minimization of flow losses was paramount in the design of Device 6, which presents only three restrictions to normal air flow. The internal chamber was initially given a crude airfoil shape to minimize turbulence, but no attempt was made to improve this shape due to funding and time constraints.

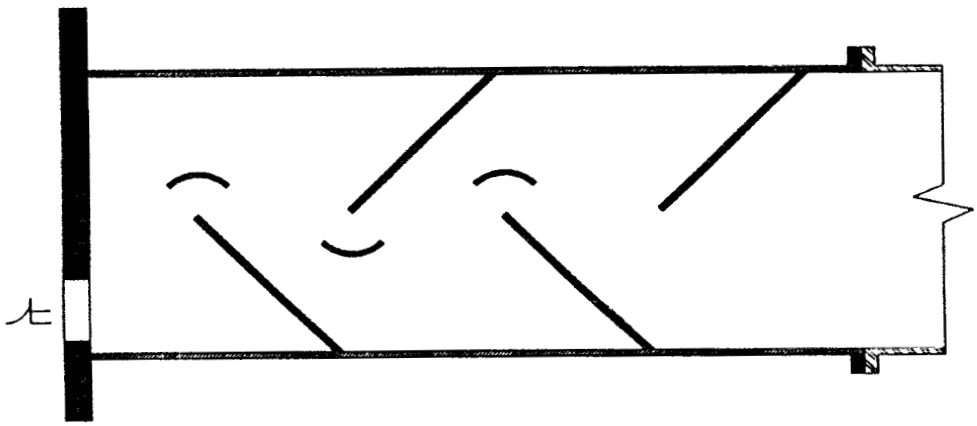

Figure 15. Device 5 with Turning Vanes

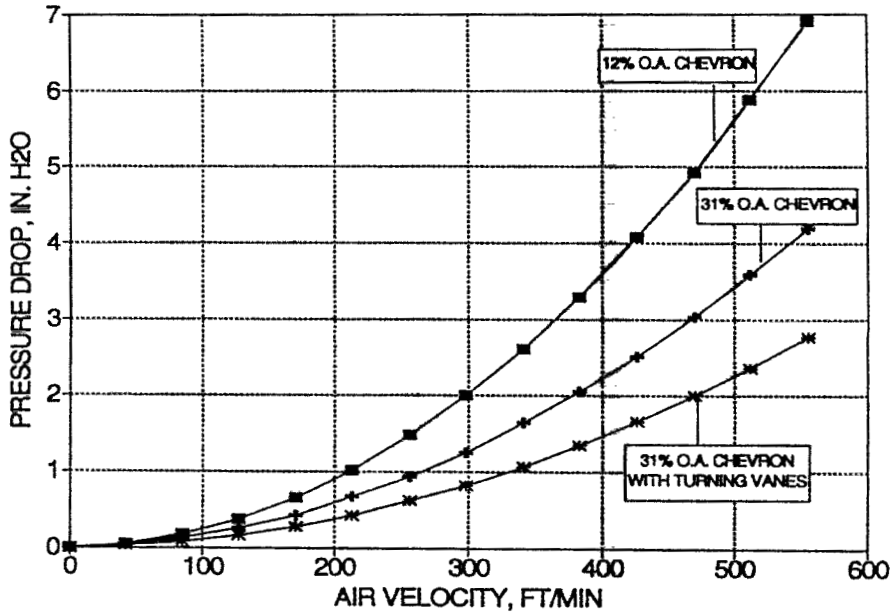

Figure 16. Pressure Drop Through Device 5; 12% Open Area, 31% Open Area, and 31% Open Area with Turning Vanes

Table 3. Airblast Attenuation of Device 5, the Chevron Model

Front Plate Vent Area (%)	Internal Plate Vent Area (%)	Shock Attenuation (%) 48-In. Standoff		Shock Attenuation (%) 77-In. Standoff	
		Pressure	Impulse	Pressure	Impulse
17.8	31.0	81.2	77.1	83.6	80.9

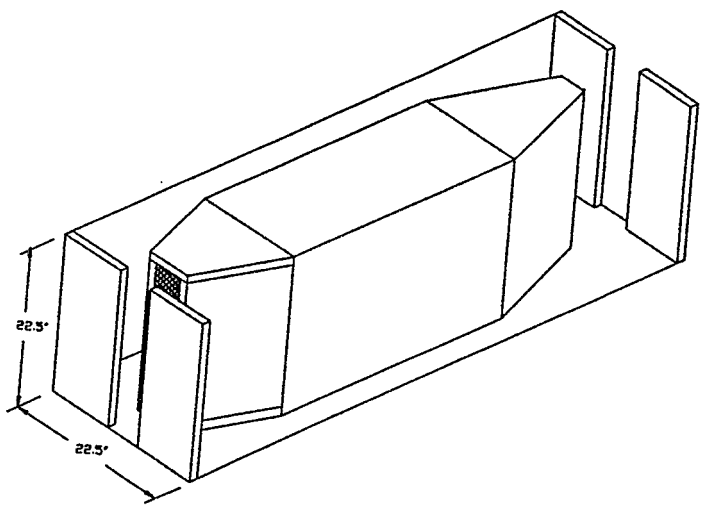

Figure 17. Configuration of Device 6 (Top and Right Walls Removed)

Device 6 was optimized for flow performance before attempting airblast attenuation tests. Airblast attenuation tests were then conducted, with modifications being limited to those items which did not affect flow loss performance.

Several flow loss test series were conducted on this model to determine optimum settings for standoff of the internal chamber behind the front plate, front plate opening width, and shock trap opening width. The ratio between front plate opening and shock trap opening was important to ensure that most of a shock wave passing through the front plate would enter the shock trap.

The final configuration had a 15.6 percent open area front plate, a standoff distance of 1.5 in. (for a 22.5 X 22.5 in. frontal area), an internal chamber mouth area of 22.2 percent., and a 22.2 percent rear orifice plate. The standoff distance provided a combined 13.3% vent area past the nose of the internal chamber. This final configuration had a measured pressure drop of 2.6 in.-H_2O at 500 ft/min, as shown in Figure 18. It is felt that the 2.0 in.-H_2O specification can easily be reached with further work to optimize the shape of the shock trap chamber to enhance smooth flow through the device.

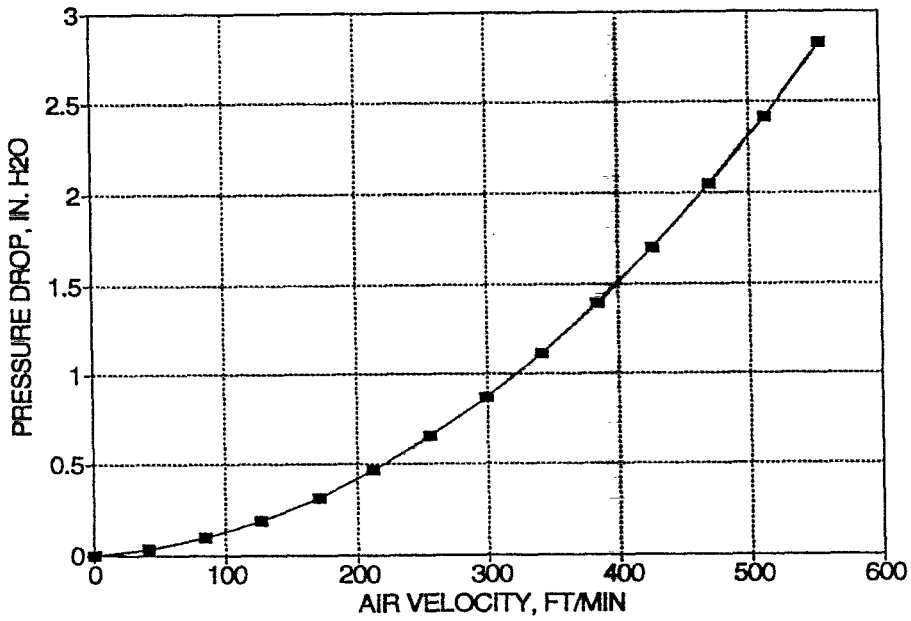

Figure 18. Pressure Drop Through Shock Trap Model, 15.6% Front Plate, 22.2% Shock Trap, 1.5-In. Standoff Distance, and 22.2% Rear Plate

An important observation made during flow loss tests was that flow stagnated across the mouth of the internal chamber. As a result, the internal configuration of the chamber has no effect on flow performance. This is a very important feature since it provides the freedom to develop a shock trap independent of air flow considerations. The following airblast attenuation tests evaluated several internal chamber designs.

A shock trap containing a converging nozzle as shown in Figure 19 was evaluated first. The results are shown in Table 4. Attenuation levels were 1 to 8 percentage points higher than any previously tested attenuator. The converging nozzle very effectively attenuated the shock reflecting out of the chamber, but this benefit was outweighed by a side-to-side reflection in the throat of the nozzle, which contributed to the initial shock that diffracted past the nose of the chamber.

The nozzle was removed from the internal chamber, resulting in an improvement in pressure and impulse attenuation at 77 in. of 2.3 and 1.3 percentage points, respectively, as shown in Table 4. The results at the 48-in. standoff were mixed, with a 0.6 point improvement in pressure attenuation, but a 0.9-point reduction in impulse attenuation.

The shock characteristics internally and downstream of Device 6 changed dramatically after removing the converging nozzle. Now, the first reflection out of the internal chamber dominated rather than the initial shock that diffracted past the nose of the chamber. It was evident that major improvements in Device 6 performance could be achieved if a means could be found to reduce the first reflection out of the internal chamber. To demonstrate the potential improvements, steel wool was loosely packed in the tail section of the internal chamber, occupying approximately

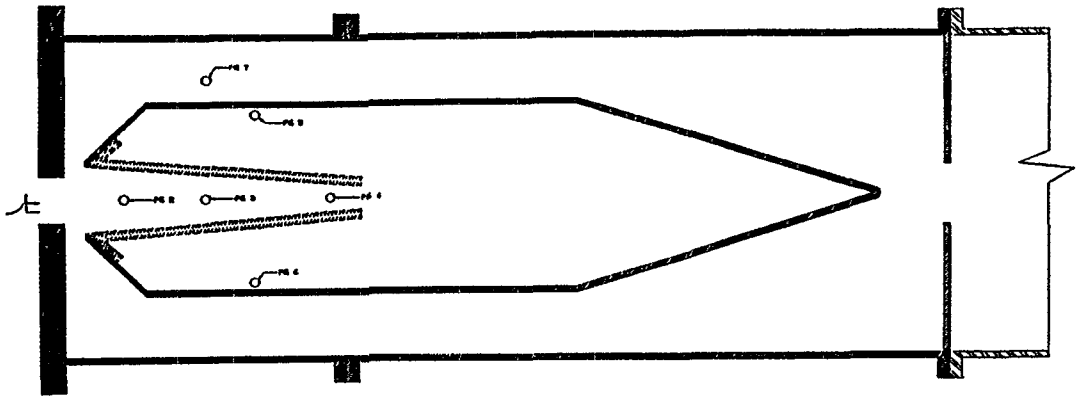

Figure 19. Device 6 Shown with Lengthened Internal Chamber

Table 4. Device 6 Shock Attenuation Test Results Using Long Internal Chamber

Internal Chamber Configuration	Shock Attenuation (%) 48-in. Standoff		Shock Attenuation (%) 77-in. Standoff	
	Pressure	Impulse	Pressure	Impulse
Converging Nozzle	83.9	85.5	86.2	88.8
Basic Design	84.5	84.6	88.5	90.1
Steel Wool in Rear 1/4	92.1	86.9	94.8	93.8

1/4 of the chamber volume. A piece of expanded metal was placed just ahead of the steel wool to keep the steel wool in place. The test results are shown in Table 4. Major improvements in attenuation were recorded. Attenuations at the 77-in. standoff were 94.8 and 93.8 percent for pressure and impulse, respectively. The numbers were not quite as high at the 48-in. standoff, with 92.1 and 86.9 percent pressure and impulse attenuation, respectively.

The first reflection from the internal chamber still dominated the downstream pressure records. This is especially true at the 48-in. charge standoff. Improvements in performance can easily be achieved through modification of the internal design of the chamber, and that attenuation levels of 96 to 97 percent are entirely feasible. Optimization of the design for flow performance will permit further reductions in opening sizes, with commensurate improvements in attenuation.

CONCLUSIONS

The feasibility of a low-cost, low-maintenance passive device was demonstrated through measurement of flow loss and airblast attenuation. Additional cost benefits will be realized in the design and construction of semi-hardened and hardened protective structures as a result of the small size of the passive devices, which have a cross-sectional area equal that of the ducting to which they are connected.

Orifice plates are the simplest passive device configuration, and this simplicity makes them inexpensive to fabricate from readily available materials. But, flow losses force the use of large orifices and dictate the plate spacing be greater than or equal to orifice width. Airblast attenuation is inversely proportional to plate spacing, so the smallest plate spacing that is acceptable from a flow loss standpoint should be used. Plate spacing was identified as a critical parameter concerning the airblast attenuation of orifice plate devices, but insufficient data were available to develop a correlation.

Two devices were designed with multiple side chambers into which shocks were directed. These devices equaled the performance of orifice plate attenuators with equal numbers of restrictions and vent areas. However, these designs were more complex, and since they did not represent a performance improvement over orifice plate designs, their added fabrication costs are not justified.

A passive device with a single chamber positioned closely behind the entrance to an attenuator proved to be very effective to accept and mitigate the preponderance of a shock wave. A design consisting of front and rear orifice plates and an elongated internal chamber achieved 92 to 95% pressure attenuation, and 87 to 94% impulse attenuation.

ACKNOWLEDGMENTS

This program was conducted for the U. S. Army Engineer Waterways Experiment Station (WES), Structures Laboratory (SL). The WES technical monitor for the contract was Mr. Gayle E. Albritton, Chief, Structural Evaluation Group (SEG), Structural Mechanics Division (SMD). The contract was funded by Headquarters, U.S. Army Corp of Engineers (HQUSACE), CERD-M.

REFERENCES

1. "PV-Blast Valves," Temet USA Inc., Blast Valve Catalogs, "TUSA PV-200-86-4 and TUSA PV-120-300-86-0.

2. "Luwa Shelter Technology," Luwa Ltd., 1989.

3. James W. Ball, J. H. Weatherly, and S. A. Kiger, "Blast Valve Effectiveness for Conventional Weapons," Waterways Experiment Station, Miscellaneous paper No. SL-92-1, February 1992.

4. Q. A. Baker, C. Y. Tuan, and W. E. Baker, "Passive Airblast Attenuation Valves for Conventional Weapons," Waterways Experiment Station Contract No. DACA39-89-C-0035, WBE Report No. WBE-124, October 31, 1989.

5. "Suppressive Shields Structural Design and Analysis Handbook," HNDM-1110-1-2, U.S. Army Corps of Engineers, Huntsville Division, Huntsville, Alabama, November 1977.

6. C. Kingery, G. Coulter, and R. Pearson, "Venting of Pressure Through Perforated Plates, Technical Report ARBRL-TR-02105, Ballistic Research Labs, Aberdeen Proving Ground, Maryland, June 1977.

7. W. E. Baker and G. A. Oldham, "Estimates of Blowdown of Quasi-Static Pressures in Vented Chambers," EM-CR-76029, Report No. 2, Edgewood Arsenal, Maryland, November 1975.

8. J. F. Proctor, "Blast Suppression/Predictive Model, WBE 4333," Monthly Technical Report, Naval Surface Weapons Center, White Oak, Silver Spring, Maryland, November 1975.

9. W. E. Baker and P. S. Westine, "Methods of Predicting Blast Loads Inside and Outside Suppressive Structures," EM-CR-76026, Report No. 5, Edgewood Arsenal, Maryland, December 1975.

10. E. D. Esparza, W. E. Baker, and G. A. Oldham, "Blast Pressures Inside and Outside Suppressive Structures," EM-CR-76042, Report No. 8, Edgewood Arsenal, Maryland, December 1975.

11. R. N. Schumacher, C. N. Kingery, and W. O. Ewing, Jr., "Airblast and Structural Response Testing of a 1/4 Scale Category I Suppressive Shield," BRL Memorandum Report No. 2623, USA Ballistic Research Laboratories, Aberdeen Proving Ground, Maryland, May 1976.

12. A. Celmins, "Analysis of Category I Suppressive Shield Effectivity Data," BRL Report No. 1936, USA Ballistic Research Labs, Aberdeen Proving Ground, Maryland, September 1976.

13. R. N. Schumacher, "Airblast and Structural Response Testing of a Prototype Category III Suppressive Shield," BRL Memorandum Report No. 2701, USA Ballistic Research Labs, Aberdeen Proving Ground, Maryland, November 1976.

14. C. N. Kingery and G. Coulter, "Shockwave Attenuation by Single Perforated Plates," BRL Memorandum Report No. 2664, USA Ballistic Research Labs, Aberdeen Proving Ground, Maryland, August 1976.

15. C. Kingery, R. Pearson, and G. Coulter, "Shock Wave Attenuation by Perforated Plates with Various Hole Sizes," BRL Memorandum Report No. 2757, USA Ballistic Research labs, Aberdeen Proving Ground, Maryland, June 1977.

16. F. H. Oertel, Jr., "Evaluation of Simple Models for the Attenuation of Shock Waves by Vented Plates," BRL Report No. 1906, USA Ballistic Research Labs, Aberdeen Proving Ground, Maryland, August 1976.

17. J. D. Renick, K. L. Kloepple, and R. W. Robey, "Evaluation of Passive Blast Attenuation Devices," Phillips Laboratory, Report No. PL-TR-91-1052, October 1991.

18. J. R. Britt and C. D. Little, Jr., "Airblast Attenuation in Entranceways and Other Typical Components of Structures. Small-Scale Tests Data Report 1," WES/TR/SL-84-22, U.S. Army Waterways Experiment Station, Mississippi, December 1984.

19. D. W. Hyde, "NATO Semi-Hardened Facility Test," Technical Report ESL-TR-89-06, U.S. Air Force Engineering and Services Center, Tyndall AFB, FL, June 1989.